Dyes and Pigments 83 (2009) 281–290

Contents lists available at ScienceDirect

Dyes and Pigments

journal homepage: www.elsevier.com/locate/dyepig

Spectroscopic and photoelectric investigations of resonance effects in selected sulfonated phthalocyanines

A. Siejak [a], D. Wróbel [a,*], P. Siejak [a], B. Olejarz [a], R.M. Ion [b]

[a] Institute of Physics, Faculty of Technical Physics, Poznan University of Technology, Nieszawska 13A, 60-965 Poznań, Poland
[b] ICECHIM-Bucharest, Analytical Department, 202 Splaiul Independentei, Bucharest, Romania

ARTICLE INFO

Article history:
Received 31 January 2009
Received in revised form
4 May 2009
Accepted 8 May 2009
Available online 11 June 2009

Keywords:
Sulfonated phthalocyanine
Electronic spectroscopy
Photoacoustic spectroscopy
Thermal deactivation
Triplet population
Photocurrent generation
Mesomeric effect
Inductive effect

ABSTRACT

Zinc phthalocyanine dyes, which had been symmetrically and asymmetrically substituted with sulfonate groups were investigated using absorption, fluorescence and photoacoustic spectroscopic methods, supported by light-induced optoacoustic spectroscopy and photoelectric measurements; unsubstituted zinc phthalocyanine was employed as reference. Fluorescence quantum yields were determined on the basis of absorption and fluorescence spectra, whereas thermal parameters as well as the yield of triplet state population and the kinetics of thermal relaxation at microsecond intervals were determined using with photoacoustic methods. The effect of the sulfonate groups on photocurrent generation was discussed in terms of the dye's molecular structure and resonance (mesomeric, inductive, steric) effects. Sulfonation of zinc phthalocyanine changed markedly its absorption and fluorescence properties owing to redistribution of the electron density within the molecule as a result of both mesomeric and inductive effects, although other effects cannot be excluded. The enhanced light-generated photocurrent observed for phthalocyanine with two sulfonate groups is explained in terms of mesomeric effects, whereas in phthalocyanine with three and four sulfonate groups, inductive effects are essential and lead to photocurrent decline.

1. Introduction

Because of the low cost and easiness in construction, organic materials are considered a perfect alternative to inorganic ones. The most versatile organic materials are porphyrin and phthalocyanine dyes that can find practical applications in various fields of technology and science like for example: photonics (new organic solar cells, molecular optoelectronics, non-linear optical materials), photomedicine (photodynamic diagnosis and therapy of cancer) and photosynthesis (in modelling of electron transfer and charge separation phenomena in reaction centres) especially due to their high absorption coefficient, easy molecular structure modification by chemical procedure and efficient photoactivity as photoconverters.

A series of free-based porphyrins and phthalocyanine dyes and their derivatives complexed with various metallic ions and substituted with different peripheral groups, chains and molecules were studied for diverse purposes [1–7]. Metallic porphyrins and phthalocyanines are of crucial importance in development of a new generation of solar cells. Recently, much effort has been devoted to optimization of photocells and it has been shown that the use of magnesium and zinc porphyrin or phthalocyanine dyes in systems which convert light energy into electric energy leads to enhancement of photocurrent in photoelectrochemical devices relative to those on free-base dyes or dyes complexed with other metal ions [8–11].

Thus in this paper we use a group of sulfonated phthalocyanines which are substituted by sulfo groups to the indole units of the dye main molecular core. The main idea of this study is to correlate spectral properties of the phthalocyanine dyes investigated and their photoelectric behavior in a photoelectrochemical cell. It has been shown that electron-withdrawing and electron-donating substituents have essential influence on spectral and electronic behavior of many organic molecules [11,12]. For example halogenated porphyrins and phthalocyanines can influence both spectral features and electric properties [13–15] due to strong resonance effects between electronegative atoms attached to the indole units and the π-electrons in the molecular macroring. However, the molecular effects of sulfo substituents on photophysical properties of the organics are rather still little known [16].

Abbreviations: ZnPc, Zinc phthalocyanine; PAS, Photoacoustic spectroscopy/spectra; BCP, Bromocresol purple; LIOAS, Light-induced optoacoustic spectroscopy; PEC, Photoelectrochemical cell; DMSO, Dimethylsulfoxide.

* Corresponding author.
E-mail address: wrobel@phys.put.poznan.pl (D. Wróbel).

0143-7208/$ – see front matter © 2009 Elsevier Ltd. All rights reserved.
doi:10.1016/j.dyepig.2009.05.013

The influence of the substituents in organic dyes can be considered in terms of the mesomeric [17,18], inductive [19–23] and/or steric [24,25] effects.

To address our task and to relate spectroscopic and photoelectric results to the resonance effects in zinc phthalocyanine without substituents, symmetrically or asymmetrically substituted with the sulfo groups, we have used the absorption, fluorescence, steady-state photoacoustics and light-induced optoacoustic spectroscopy and photocurrent generation kinetics examinations.

2. Materials and methods

2.1. Dyes

The molecular structure of the dyes is shown in Fig. 1. In our experiments we used two symmetrically substituted dyes (**2**, **4**) and one asymmetric phthalocyanine dye (**3**). The ZnPc dye without substituents (**1**) was used as a standard sample. The dyes were dissolved in dimethylsulfoxide (DMSO) and the concentrations were 10^{-5} M for absorption and fluorescence measurements or 10^{-3} M in photoacoustic and photoelectric experiments.

A stock solution in DMSO (10^{-3} M) was prepared by the use of a powdered component of known molecular weight. Then, the samples were diluted in DMSO to required concentrations.

2.1.1. Synthesis of sulfonated ZnPc

Synthesis of sulfonated zinc phthalocyanine (ZnPc) was based on the modified method reported by Ambroz et al. and Dixon et al. [26,27]. Fuming sulfuric acid was added dropwise to ZnPc. The sulfonation process was carried out in the four necked glass flasks, heated in an oil bath and equipped with a reflux cooler, agitator and thermometer and with a dosing funnel. 300 g of fuming sulfuric (consisting of 30% SO_3) acid was charged into the flask and subsequently 30 g of ZnPc was gradually charged through the dosing funnel into agitated fuming sulfuric acid. The mixture was agitated at 30 °C until all ZnPc was fully dissolved. After that, the dosing funnel was removed and an inlet of nitrogen was installed instead of it. The process of sulfonation was carried out under a nitrogen blanket. The reaction mixture was agitated and heated up to a temperature between 115 and 125 °C, and subsequently kept in adjusted temperature for 30 min.

The concentration of fuming sulfuric acid and temperature of the sulfonation were chosen according for the target level of sulfonation. Lower sulfonated (mostly mono- and di-sulfonated) phthalocyanines were obtained when 5% fuming sulfuric acid was used at the temperature of 115 °C, whereas higher sulfonated (mostly di- and tri-sulfonated) phthalocyanines were obtained with 6% fuming sulfuric acid, at 125 °C. In the former case, the final product contained ca. 36% of mono- and 53% of di-substituted phthalocyanine, whereas in the latter, the contents of di- and tri-sulfonated phthalocyanines amounted to 28% and 54%, respectively. The mixture was stirred rapidly and maintained at 100 °C for 25 min. After the sulfonation process was terminated, the reaction mixture was slowly cooled down to laboratory temperature and subsequently charged with a dropping funnel into the vigorously agitated mixture of 2000 g of ice and 1000 g of water. Then the water suspension was filtered with a Buchner funnel, the filter cake was washed with distilled water until no sulfate anions were detectable in the filtrate. Thoroughly washed filter cake of sulfonated ZnPc was dried in a laboratory dryer at 105 °C to a constant weight.

The contents of particular sulfonated ZnPc were determined by HPLC (see below). The dry product of sulfonation was always a mixture of mono-, di-, tri- and tetra-sulfonated ZnPc. In order to obtain mono-, di-, tri- and tetra-sulfonated ZnPc, the mixtures of sulfonated derivatives, prepared as described above, were separated by the column liquid chromatography. The glass chromatographic column was filled with silica gel (Kieselgel 60 Merck), the mixture of ethyl acetate, ethanol and 25% ammonia water (in the volume ratios 7:4:4) was used as a mobile phase. The purity of each dry product was determined by HPLC method, IR data [KBr (ν_{max}/cm^{-1})]: 3223 (O–H), 1735, 1624 and 1566 (C=C), 1394 (C–N), 1228, 1166 and 1087 (C–H), 1026 (S=O), 985, 895, 741 and 721 (C–H) and UV–Vis (water, pH 7) [28–30].

2.1.2. Chromatographic analysis

The mixtures of sulfonated phthalocyanines were assayed by analytical HPLC using a reverse-phase column, gradient elution with a methanol-phosphate buffer and UV absorption spectroscopy. A programmable Beckman 420 controller was used to drive two Beckman Altex 11OA pumps; one pumping methanol and the other one 10 mM aqueous phosphate buffer adjusted to pH 5.0. The output from the pump was mixed in a home-built low volume mixing unit before passing through the injection unit. Separation was achieved using a pre-column (Waters Guard-Pak Resolve C_{18}) and a compressed column (Waters Novo-Pak 8 × 100 mm in Waters 810 RCM) and the effluent was analyzed using a Beckman 410 UV absorption detector operating at 365 nm and recorded on a chart recorder.

In a typical analysis 1 mg of the sample was dissolved in 2 ml of buffer and filtered (Millipore, 0.22 pm). The aliquot (20 μl) was

1. **ZnPc** – where R_1-R_4=H

2. **ZnPc(SO_3^{2-})$_2$** – where R1, R3=(SO_3^{2-}); R_2, R_4=H

3. **ZnPc(SO_3^{2-})$_3$** – where R_1- R_3=(SO_3^{2-}); R_4=H

4. **ZnPc(SO_3^{2-})$_4$** – where R_1– R_4=(SO_3^{2-});

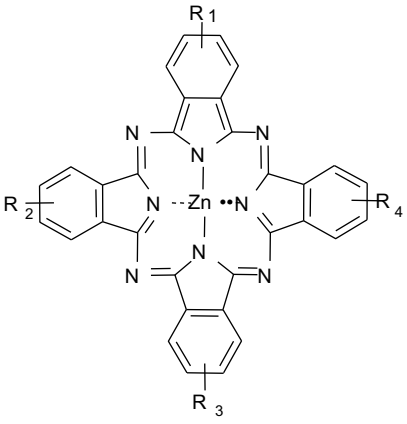

Fig. 1. Molecular structure of zinc phthalocyanine and sulfonated zinc phthalocyanines under study.

injected onto the column equilibrated with the 100% buffer at 2 ml/min. The solvent was changed to a mixture of 20% buffer and 80% methanol over a period of 18 min. During this period the fractions of sulfonated phthalocyanines were eluted. Large-scale separations were carried out on a medium-pressure chromatography column. A 25 mm × 150 mm column was packed with C_{18} silica gel and water, methanol; the mixture was pumped at 10 ml/min. The sulfonated mixture (less than 1 g) was dissolved in 10 ml of water and injected onto the column which was eluted with water for 1 h. During this period, the tri- and tetra-sulfonated components were washed off the column and analyzed by HPLC. The mono-, di-components were sequentially eluted with aqueous methanol.

2.2. Spectroscopic methods

Electronic absorption spectra were measured with a Cary 4000 (Varian, USA) in the range of 300–800 nm. Steady-state fluorescence measurements were done with a fluorometer Hitachi F4500 (Japan) in the range of 600–850 nm. Fluorescence was excited at about 350 nm and 620 nm and performed in an L-geometry set-up. Absorption and fluorescence measurements were done in a quartz cuvette at room temperature.

Relative fluorescence quantum yield was estimated on the basis of the absorption and fluorescence spectra according to the method described elsewhere [31,32] with the following equation:

$$\Phi_F = \Phi_R \frac{I}{I_R} \frac{A_R}{A} \frac{n^2}{n_R^2}, \quad (1)$$

where Φ_R is the fluorescence quantum yield of a reference sample (ZnPc), I and I_R are the integrated fluorescence of the sample and reference, respectively, A and A_R are the fraction of light absorbed by the sample and reference, respectively and n and n_R are the refractive indices for the sample and reference, respectively.

The steady-state photoacoustic spectra were registered with a single-beam photoacoustic spectrometer PAC 300 (MTEC, Iowa, USA) and three modulation frequencies were applied (8, 15, and 30 Hz) at a constant phase shift. The samples were located in a photoacoustic chamber filled with helium gas and a signal was detected with a very sensitive microphone. A black material was used for correction of the device response [33]. The measurements were performed at 20 °C.

Gaussian analysis used for the absorption and photoacoustic spectra was performed with an Origin Pro 7.5 Peak Fitting program.

Triplet state population and its thermal relaxation were monitored with the light-induced optoacoustic spectroscopy (LIOAS) [34] and the samples were illuminated by a flash from the GL-3300/Gl301 nitrogen laser (Photon Technology Int.), combined with the dye laser (λ_{ex} = 415 nm) of a pulse duration of 0.2 ns. The time resolution of the LIOAS apparatus was 0.4 μs. A thermal reference sample used in the LIOAS experiments was bromocresol purple (BCP) dissolved in DMSO which is supposed to change whole absorbed energy into heat in the time shorter than the LIOAS device time resolution. The photothermal experiments were done in helium atmosphere at 20 °C and the samples were located in a thermally stable cuvette. The details of the experimental set-up and of analysis of the LIOAS signals were described in [35–37]. The yield of triplet state population Φ_T was evaluated using the following equation [35]:

$$\Phi_T = \frac{(1-\alpha)E_{hv} - \Phi_F E_F - \Phi_D E_D}{E_T}, \quad (2)$$

where α is a part of energy changed into heat in a time shorter than the resolution time of the LIOAS device (α is supposed to be 1 for the thermal standard sample BCP), E_{hv} is the molar energy of the incident photons (evaluated for 415 nm), Φ_F is the fluorescence quantum yield, E_F and E_T are the energies of the fluorescence and the triplet states, Φ_D and E_D are the quantum yield and energy, respectively, of additional effects which could occur after excitation and are not measurable directly with our equipment (except fluorescence, internal conversion and intersystem crossing). The α parameter for the sample is estimated from the maximal LIOAS H signal of a sample using equation [36]:

$$H = k\alpha E_L(1 - 10^{-A}), \quad (3)$$

where k is a geometrical and electrical set-up factor of the device, A is absorbance of the sample and E_L is energy of the laser.

Kinetics parameters of thermal relaxation of the triplet state were evaluated with the procedure proposed by Rudzki-Small et al. [37]:

$$H(t) = r(t)\sum_i k_i \exp\left(-\frac{t}{\tau_i}\right), \quad (4)$$

where $r(t)$ is the weight factor of deconvolution, k_i is a pre-exponential factor, τ_i is the lifetime of the i-th transient.

2.3. Photoelectrical experiments

The kinetics of photocurrent generated (in the second–time scale) were recorded in a photoelectrochemical cell (PEC) constructed of semiconductor (In_2O_3) and gold electrodes distanced with a 60 μm Teflon® spacer with the use of an automatic potentiostat–galvanostat (Compex, Poland) in the short circuit condition. The dye in PEC was excited with white light with a xenon lamp XBO 500 (25 mW/cm^2) from the semiconductor electrode side; the details of the photo-device and measurements can be found in [38]. A water filter and the glass filter (BC10) were used to cut off UV and IR radiation.

3. Results and discussion

3.1. Electronic absorption and fluorescence studies

Fig. 2 shows the electronic absorption spectra of all dyes investigated dissolved in DMSO. The shape of the spectrum of **1** is characteristic of ZnPc and somewhat different from that found in literature [4,25,38] because of the use of DMSO as a solvent. Four bands are well recognized; in the Soret region a band with a peak at 350 (not shown) nm, and the remaining bands in the Q region at 607 nm and 642 nm (low intensive) and at 672 nm (very intensive). The marked changes in the spectra shapes and in the ratios of the bands' intensities are evidently observed when ZnPc is substituted with sulfo groups, but in different manner depending on the number of attached groups and symmetry of the dye molecular structure after substitution. In the spectra of substituted phthalocyanine dyes the Soret bands are shifted (from 5 to 14 nm – Fig. 2). The more spectacular changes are seen in the Q regions. First of all the main Q band observed at 672 nm in the spectrum of standard sample **1** is shifted to the long-wavelengths in the spectra of sulfonated dyes (681 nm–685 nm depending on the dye). However, in all substituted phthalocyanines the bands in the range of 707–710 nm are present and the intensity ratios of the main Q band (at 681 nm in **2**, **4**; at 685 nm in **3**) to the 707–710 nm band change and depend on the dye molecular structure and symmetry. The Gaussian analysis in the Q range evidently shows three components of the absorption bands of **1** and four components of the relevant bands of **2**–**4**. This result indicates a strong influence of the sulfo

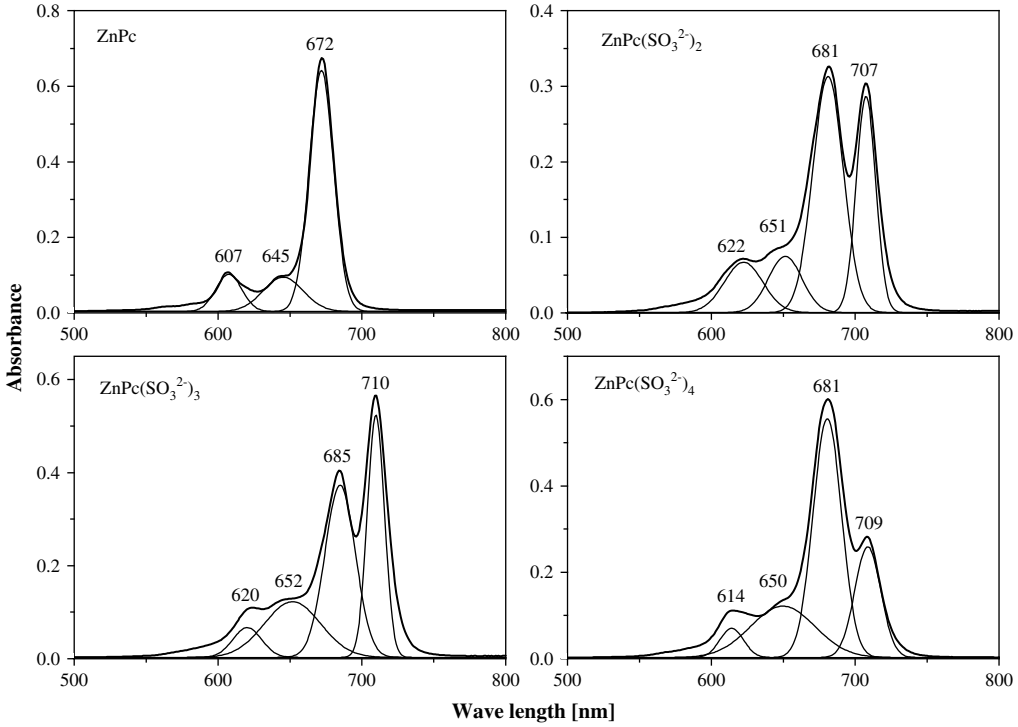

Fig. 2. Absorption spectra of zinc phthalocyanine (ZnPc) and sulfonated zinc phthalocyanines (ZnPc(SO_3^{2-})$_{2-4}$) in DMSO; ($c = 10^{-5}$ M). Gaussian components are also shown. (residuum = 0.01 ÷ 0.05).

groups on the absorption features of the dyes. On the basis of Gaussian analysis the dyes' absorption parameters are evaluated and collected in Table 1. The changes observed in the dyes' absorption spectra upon sulfonation could be explained as due to formation of small aggregates and occurrence of a new transition with lowering energy upon substitution with the sulfo groups.

The red shifts of the absorption bands can be related to several effects: aggregation, charge transfer complexes, point charges and others [39–41]. Sulfonated phthalocyanines are well known to form some aggregated species [42–44]. However, they can dimerize easily in aqueous solutions. Thus, the influence of the aqueous surrounding is very much different from that of the solvent used in our experiments. Dimerization could be avoided by the use of a proper solvent (e.g. highly polar DMSO) and samples of low concentration as we did. Our main idea was to use very low concentrated samples to avoid (or at least to minimize) the presence of aggregates in our samples in the spectroscopic experiments. The presence of aggregates may interfere with the subtle resonance effects. Therefore we used samples of a very low concentration (10^{-5} M) in polar DMSO. The use of 10^{-5} M samples can guarantee detection of sufficiently strong signals to be observed and to follow resonance effects when they appear. The presence of the band at about 630 nm could indicate the appearance of some aggregated structures [28,45]. However, the intensity of the 630 nm band is much lower than that at nearly 680 nm. When some aggregated forms dominate (like for example when sulfonated phthalocyanines was studied in water against DMF [28] and in water *versus* in water after treatment with Triton X-100 [45]) one should observe a great change in the intensity ratios of the band at 630 *versus* that at 680 nm. This is not the case for our samples.

The existence of some aggregated structures of the dyes cannot be excluded even when polar DMSO is used as a solvent to protect against dimerization. The tendency towards aggregation of sulfonated copper phthalocyanines was noted even at low concentrations of hydrous solvent applied [46]. However, in DMSO we have strong domination of monomeric forms as seen from

Table 1
Absorption parameters of zinc phthalocyanine (ZnPc) and sulfonated zinc phthalocyanines (ZnPc(SO_3^{2-})$_{2-4}$ in DMSO; $c = 10^{-5}$ M.

Dye	λ^A_{max} [nm]				ε (λ_{max}) × 10^5 [M^{-1} cm^{-1}]			Absorbance ratio			
	S	Q_1	Q_2	Q_3	S	Q_2	Q_3	S/Q_2	S/Q_3	Q_1/Q_2	Q_2/Q_3
ZnPc	350	607	672	–	0.16	0.64	–	0.26	–	0.16	–
ZnPc(SO_3^{-2})$_2$	355	622	682	707	0.13	0.31	0.29	0.42	0.45	0.22	1.09
ZnPc(SO_3^{-2})$_3$	364	624	684	710	0.16	0.37	0.52	0.44	0.32	0.18	0.71
ZnPc(SO_3^{-2})$_4$	355	615	681	708	0.29	0.55	0.26	0.53	1.13	0.13	2.14

FWHM [cm^{-1}]		$\Delta\lambda$ [cm^{-1}]		
Q_2	Q_3	S	Q_2	Q_3–Q_2
440	–	–	–	–
570	310	200	740	540
510	270	280	800	510
520	430	200	780	580

S – Soret band, Q_1, Q_2, Q_3, – Bands in the Q region, ε (λ_{max}) – Molar absorption coefficient in the maximum of the bands ($\Delta\varepsilon = \pm 0.01 \times 10^5$ [M^{-1} cm^{-1}]), FWHM – Half width at half magnitude (ΔFWHM = 10 cm^{-1}), $\Delta\lambda$ – Band shift ($\Delta(\Delta\lambda)$ = 10 cm^{-1}).

our absorption and fluorescence experiments. Changes in the absorption spectra of the dyes after sulfonation manifested in the relations of intensities of the bands at 681 nm (in **2**, **4**) or 685 nm (in **3**) with respect to those of the new band with the maximum at 707–710 nm (in **2**, **3**, **4**) evidently indicate some modifications in the dye electronic structure. This supposition is supported also by changes in the molar absorption coefficients of the dyes. As shown, variations in the absorption band intensities and band locations are due to the presence of sulfo groups attached to the main phthalocyanine core. On the basis of the absorption experiments it is evident that the presence of the external sulfo groups modifies distribution of π-electrons in the phthalocyanine macroring. Thus we have every reason to believe that the bands at 707–710 nm in **2**–**4** could be attributed to the additional energy transition owing to the presence of the sulfo substituents. Modification in the spectral parameters of samples **2**–**4** with respect to those of their counterpart **1** shown in this paper was also found for other symmetric halogenated phthalocyanines: fluorinated $ZnPcF_{16}$ [11] as well $CuPcF_{16}$ and $CuPcCl_{16}$ [12], however the spectral character of the halogenated phthalocyanines was different. In our experiments presented in this paper we use phthalocyanine ZnPc substituted with the sulfo groups. These groups attached have ionic character and thus can strongly influence the dyes' features [11,46]. The sulfo substituents cause a decrease in the molar absorption coefficients in the Q region of the spectra of samples (**2**–**4**) with respect to that in the spectrum of the maternal sample **1** and thus we could suppose the existence of the mesomeric and/or inductive effects.

Electronic properties of aromatic compounds can be also influenced by point charges, changes in molecular conformation and steric effects. According to literature data [39,47,48] the evidence is well seen in some porphyrins (e.g. chlorophylls and bacteriochlorophylls or their derivatives) and concerns pigment–protein complexes. The negative charge coming from the attached sulfo groups is able to give a red shift of the absorption spectrum of large magnitude of the complexes in aqueous media. A point charge effect is very strongly affected by the molecular structure of a dye and its environment. In [39] the red shift was assigned to a point charge of chlorophyll in polar amino acid. For porphyrin dyes the red shift is expected to range from about 200 cm^{-1} to about 2700 cm^{-1} *versus* monomer [49,50] and could be assigned at least partially to a point charge shift. In this paper the red shifts of 200–280 cm^{-1} (the Soret band), of about 800 cm^{-1} and of 510–580 cm^{-1} (the Q region) are observed (Table 1). However, we have observed not only the red shift of the bands but also the extra band in the long wavelength region, near about 700 nm. The half widths at half maximum (FWHM) values of these bands range from 270 to 570 cm^{-1} *versus* 440 cm^{-1} in **1** (Table 1). Of course, the effect of a point charge cannot be excluded, nevertheless at this stage of the study we are not able to judge how weak or strong is the influence of a point charge on the observables.

The dyes under study emit fluorescence and their fluorescence spectra are shown in Fig. 3. Their shape as well as location of the fluorescence bands (679 nm – main band, and 742 nm (much less intense band with a hump at about 708 nm) of the standard sample **1** are similar to that found in literature [4,46]. However, the shapes of the fluorescence spectra of **2**–**4** are markedly modified in the presence of sulfo substituents. The fluorescence quantum yields of the substituted dyes (Eq. (1)) change insignificantly (Φ_F = 0.12–0.16) with respect to that for the reference **1** (0.18). The details of the basic fluorescence parameters evaluated for excitation in the Q band region (~620 nm) are collected in Table 2. The fluorescence spectra for **1** are independent of the excitation wavelength. The spectra obtained for **2**–**4** show some small differences.

In this paragraph we will concentrate on the origin of emission and the reason for the band shift. The origin of the band's shift is rather obvious; it is the redistribution of electron density in the main π–π* molecular structure of the phthalocyanines investigated upon sulfonation. The above interpretation is in agreement with

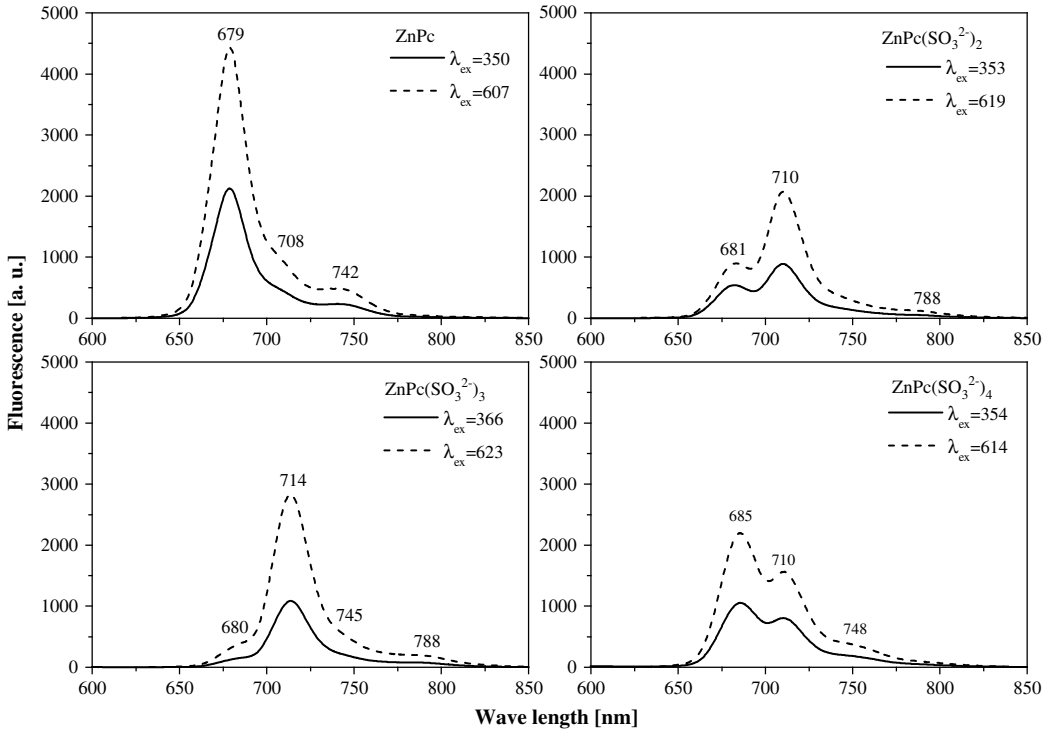

Fig. 3. Fluorescence spectra of zinc phthalocyanine (ZnPc) and sulfonated zinc phthalocyanines ($ZnPc(SO_3^{2-})_{2-4}$) in DMSO, λ_{ex} = ~620 nm; ($c = 10^{-5}$ M).

Table 2
Fluorescence parameters of zinc phthalocyanine (ZnPc) and sulfonated zinc phthalocyanines ($ZnPc(SO_3^{2-})_{2-4}$ in DMSO; $c = 10^{-5}$ M.

Dye	λ^F_{max} [nm]			Fluorescence ratio			Φ_F
	F_1	F_2	F_3	F_1/F_2	F_1/F_3	F_2/F_3	
ZnPc	679	708	742	4.52	9.21	2.04	0.18*
$ZnPc(SO_3^{-2})_2$	681	710	–	0.43	–	–	0.16
$ZnPc(SO_3^{-2})_3$	680	714	745	0.13	0.70	5.22	0.12
$ZnPc(SO_3^{-2})_4$	685	710	748	1.40	6.16	4.38	0.12

F_1, F_2, F_3, – Fluorescence bands, Φ_F – Fluorescence quantum yield, * – From [67], $\Delta\Phi_F = \pm 0.01$. The details of the fluorescence parameters evaluated for excitation in the Q band region (~620 nm).

the observations in the absorption spectra and our supposition as to the occurrence of the resonance effects caused by an influence of the sulfo groups attached to the porphyrazine ring.

The question arises as to the differences in the fluorescence spectra of the samples investigated. The differences between the emission of **1** and those of the remaining dyes (**2**–**4**) are due to the presence of the sulfo groups and could be attributed to the resonance effects leading to a modification in the molecular electron density. Moreover, it is worth noting some differences in the fluorescence behavior of the substituted dyes. The differences could be discussed in terms of: (i) differences in the molecular symmetry of the dyes and (ii) the origin of the fluorescence bands. The dye molecules differ in the number of the sulfo groups. The changes in the molecular structure lead to the changes in molecular symmetry. ZnPc (sample **1**) is characterized by D_{4h} symmetry (covalent and coordinated bonding in the metallic phthalocyanines could break the D_{4h} conjugated system symmetry or lead to an asymmetry), and the symmetry is disturbed after sulfo group's attachment. Sample **4** has four groups and the symmetry of the molecule is also D_{4h}; however its fluorescence spectrum is perturbed by the presence of four sulfo groups and the intensity of the band at 709 nm is even markedly higher than that of the corresponding band in the spectrum of **1**. Sample **2** has two groups attached and its symmetry is D_{2h}, thus in this compound electron distribution is strongly modified when compared to that of sample **4**. The spectrum of sample **3** with three sulfo groups attached differs from those of **2** and **4**.

The origin of fluorescence in the range from 650 nm to about 750 nm can be discussed as coming from the Q-band transitions and some transient species [4,11,46,51,52]. The Q-band transitions overlapped by the emission of some transient species were observed in some sulfonated phthalocyanines derivates [52] and other aromatic dyes with anionic groups [53]. The origin and nature of the transient species is not fully clear as yet, however according to the discussion based on the Raman and fluorescence data [52] the band in the range 650–750 nm assigned to the Q-band emission is also covered by the emission of transient species. Thus, the bands at 710 nm (**2**, **4**) and 714 nm (**3**) can be interpreted as the Q-transition fluorescence overlapped with the emission of some minor intermediates (emission effect of the latter is out of the scope of this contribution). However, these bands in the spectra of **2**, **3** and **4** are intensive and slightly bathochromically shifted with respect to the fluorescence emission bands in the spectrum of basic ZnPc (**1**). This spectral modification is clearly seen and its source could be assigned not only to the presence of a small amount of the transition species (if any) but predominantly to the changes in electronic redistribution affected by the sulfo groups attached to the indole units and the resonance interaction with the porphyrazine ring.

The above interpretation can be verified by analysis of the excitation emission spectra. We observed these excitation spectra in the spectral range beyond 700 nm to monitor all species which could contribute to fluorescence in this region (Fig. 4). The spectrum of **1** coincides very well with that of absorption as expected for the monomeric dye. The absorption and excitation emission spectra of **3** and **4** are also similar, although the relations between the emission signals are a little bit changed with respect to those in the absorption spectra. The exception is the spectrum of **2** in which the inversion of the band's intensity in the Q region (when comparing the spectra of absorption and excitation) is well seen. The results indicate that sample **2** and the remaining sulfonated

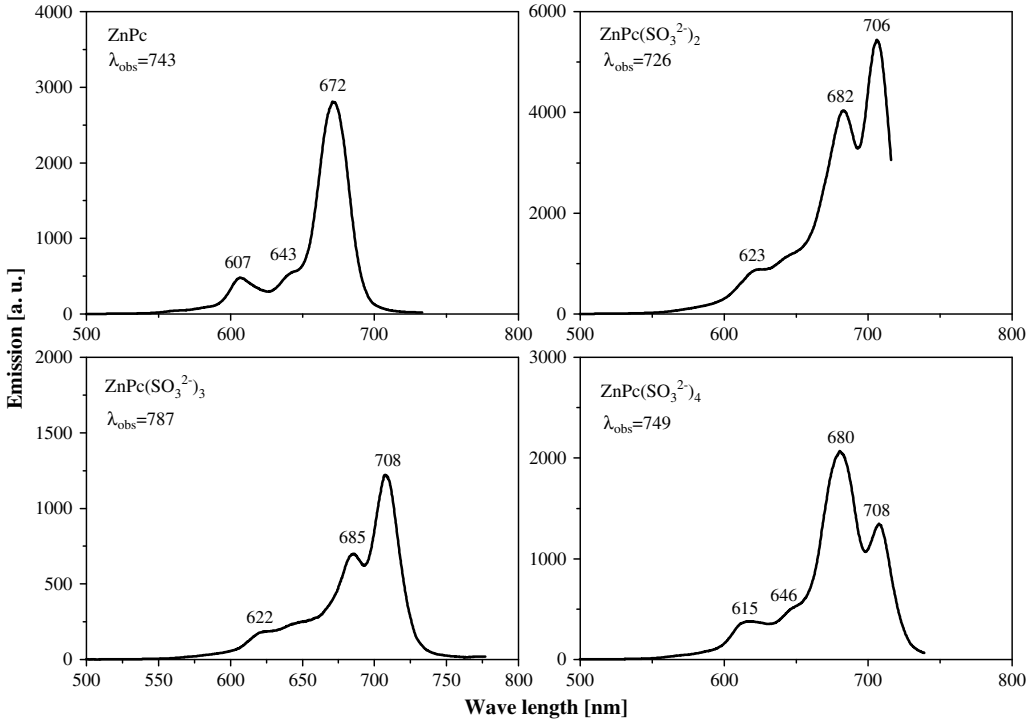

Fig. 4. Excitation emission spectra of zinc phthalocyanine (ZnPc) and sulfonated zinc phthalocyanines ($ZnPc(SO_3^{2-})_{2-4}$) in DMSO, $\lambda_{obs} > 700$ nm; ($c = 10^{-5}$ M).

samples (**3** and **4**) have different channels of deactivation. The differences in the photophysical behavior may be related to at least two reasons: (i) a number of the sulfo groups and different dye molecular structures, and (ii) different molecular symmetry of the dyes. These effects can contribute to this different spectral features and lead to other ways of deactivation like e.g. non-radiative transitions. The results on the non-radiative deactivation way following from our photothermal examinations are presented below.

3.2. Photothermal property studies

To date little is known about the influence of the sulfo groups on dye thermal deactivation. The photoacoustic spectra in the range of 500–800 nm are shown in Fig. 5 (the data for one light modulation frequency (20 Hz) are presented as an example). Photoacoustic examinations give information about global thermal deactivation channels in which both the singlet and triplet states of a molecule can be involved. The results presented in Fig. 5 clearly confirm that part of the excitation energy is deactivated as a result of non-radiative internal conversion and intersystem crossing transitions. On the basis of the absorption and photoacoustic spectra we can evaluate thermal deactivation parameters (TD = PAS/A; A and PAS are absorbance and photoacoustic signals, respectively) and the data are gathered in Table 3. For evaluation of the TD parameters, the corresponding Gaussian absorption and PAS components are used. The shapes of PAS for **1**, **3** and **4** correspond very well with those of their absorption spectra. However, the exception is sample **2** for which the band at about 610 nm is much stronger in intensity and broader when compared to that of the remaining samples. The high intensity of the 610 nm band and its broadening would confirm the existence of the some species which exist only in the excited state, thus it is well seen in the excitation and PAS spectra. Also the PAS bands in the spectrum of **2** are much broader in the spectral range of 600–700 nm. The thermal deactivation parameters – TD (Table 3) evidently show that the dyes with the substituents are more effective in thermal deactivation than that in the standard **1**. Thus it is clear that the presence of the sulfo groups in the dye molecular structure changes markedly their thermal transitions. The PAS results show a correlation between the molecular structure of the dyes and their participation in thermal processes; these processes are affected by the presence of the sulfo groups. The linear correlation factors (linear least squares fit) for the PAS experimental data and theoretical prediction [54] reach the values 0.99 and confirm domination of monomeric structure of dyes in our experiments.

3.3. Thermal relaxation study

However, on the basis of our steady-state measurements we are not able to distinguish prompt and slow thermal effects. Light-induced optoacoustic spectroscopy (LIOAS) is an excellent tool for this purpose. Therefore we performed the time-resolved measurements to get the information on participation of the singlet-triplet transitions in thermal deactivation and to estimate the yield of triplet population as well as thermal relaxation decay.

The dyes investigated show typical LIOAS wave forms (Fig. 6) as observed for other phthalocyanine dyes [12,35]. The α parameter was evaluated from Eq. (3) assuming that the k factor was the same for all dyes ($\alpha < 1$) and standard BCP (with $\alpha = 1$). The data are collected in Table 4. The values of α and k_1 parameters evaluated from Eqs. (3) and (4), respectively, are nearly the same (to the accuracy of the experiment), as expected [36,37], and they are 0.60–0.79 and 0.57–0.76, respectively. It means that more than 50% of the energy absorbed is changed into heat in thermal processes promptly, in the time duration shorter than 0.4 μs. Eq. (2) permits estimation of the yield of triplet state population. In this calculation, the Φ_F values were taken from our fluorescence study, E_T is taken from literature for similar phthalocyanine dyes [55]. The Φ_T values (0.39–0.92) depend on the dye but they are coherent with

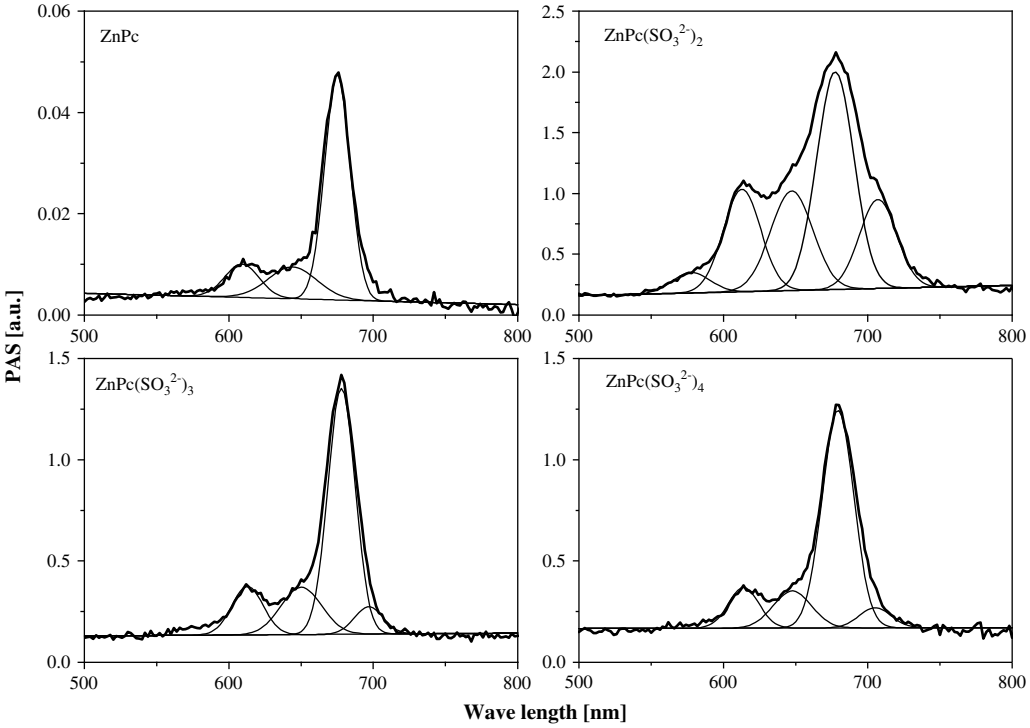

Fig. 5. Photoacoustic spectra of zinc phthalocyanine and sulfonated zinc phthalocyanines in DMSO; ($c = 10^{-3}$ M); light modulation frequency 20 Hz. Gaussian components are also shown; (residuum = 0.01 ÷ 0.05).

Table 3
Thermal deactivation parameters of zinc phthalocyanine (ZnPc) and sulfonated zinc phthalocyanines (ZnPc(SO_3^{2-})$_{2-4}$ in DMSO; $c = 10^{-3}$ M.

Dye	S	Q_1	Q_2	Q_3
ZnPc	0.1	0.1	0.1	–
ZnPc(SO_3^{-2})$_2$	11.5	14.7	6.3	3.2
ZnPc(SO_3^{-2})$_3$	2.9	3.4	3.3	0.6
ZnPc(SO_3^{-2})$_4$	2.2	2.1	2.1	0.2

S, Q_1, Q_2 , Q_3 – as in Table 1; data for $\nu = 20$ Hz; $\Delta TD = \pm 0.1$.

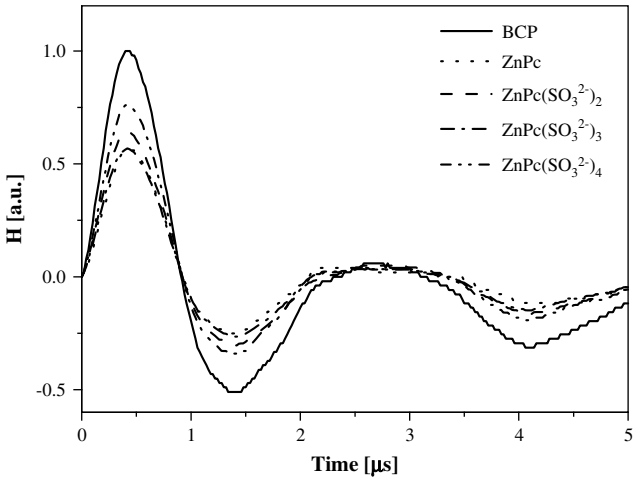

Fig. 6. The LIOAS wave forms for standard sample (PCB) and zinc phthalocyanine (ZnPc) and sulfonated zinc phthalocyanines (ZnPc(SO_3^{2-})$_{2-4}$) in DMSO; $\lambda_{ex} = 415$ nm; ($c = 10^{-3}$ M).

those for other porphyrins [55,56] and phthalocyanines [57] and the results show that all dyes studied are able to generate triplet states. For samples **2** and **4** the population of triplet states is lower than those for the remaining dyes. This result confirms that the symmetry of the dye molecules influences markedly the triplet state features. The deconvolution analysis (Eq. (4)) gives the best results for two Gaussian components with $\tau_1 \leq 0.4$ μs and τ_2 ranging from 0.76 to 1.53 μs (depending on the dye). The last result could be assigned to thermal relaxation with participation of the long-lived triplet states of the dyes. The sum of k_i ($i = 1, 2$) is less than 1 indicating that processes other than intersystem crossing in the molecules could also contribute to deactivation. These processes could be: (i) generation of singlet oxygen (it can be excluded since we perform our LIOAS experiments in nitrogen atmosphere), (ii) photochemical reaction (could not be excluded taking into account electronegative character of the substituents [46,52], however it could have a marginal role because our samples have been studied in nitrogen atmosphere), (iii) deformation of the molecular skeleton and steric effects leading to changes in conformation of a molecule, (iv) phosphorescence (in the LIOAS examination we follow thermal relaxation thus we cannot discuss this point and it will be the topic of our incoming paper), (v) perturbation in electron distribution due to intermolecular electron transfer occurring in the dyes with the attached sulfo groups.

3.4. Photocurrent generation

Photocurrent generation was monitored for the dyes in PEC. The mechanism responsible for light-induced current was discussed in details in [4,11,55] and attributed to an electron injection from a dye to a semiconductor electrode [58]. Fig. 7 shows the results of photocurrent kinetics in the second time scale. As follows, the

Table 4
LIOAS results for zinc phthalocyanine (ZnPc) and sulfonated zinc phthalocyanines (ZnPc(SO_3^{2-})$_{2-4}$ in DMSO.

Dye	α	K_1	K_2	Φ_T	τ_2 [μs]
ZnPc	0.63	0.57	0.02	0.76	1.53
ZnPc(SO_3^{-2})$_2$	0.70	0.64	0.04	0.58	0.76
ZnPc(SO_3^{-2})$_3$	0.60	0.57	0.04	0.92	1.10
ZnPc(SO_3^{-2})$_4$	0.79	0.76	0.06	0.39	1.23

α – A part of excitation energy exchanged into heat promptly (in time shorter than 0.4 μs), K_1 – Pre-exponential factor for $\tau_1 = 0.4$ μs, K_2 – Pre-exponential factor and τ_2 – Decay time for the time range of 0.4–5.0 μs; $\Delta\alpha = \pm 0.06$, $\Delta\Phi_T = \pm 0.1$, $\Delta\tau_2 = \pm 0.01$.

current intensity, character of the rise and decay depend strongly on the samples which confirms that the molecular structure and the presence of the sulfo groups in the dyes investigated markedly influence the π-electron distribution. The highest current was obtained for sample **2** (about 30 nA/cm^2) when compared to those for the remaining dyes (4 nA/cm^2 for **1**, 1.5 nA/cm^2 for **3** and nearly 0 for **4**). The increase in the photocurrent in PEC with sample **2** (the dye with two sulfo groups) could indicate the presence of the mesomeric effect and its domination over the inductive one. It could be explained as follows. Thermal deactivation of this dye is high (when compared to its sulfonated counterparts) and its fluorescence quantum yield is similar to those for the remaining dyes. Thus the reason of its high photoconversion of light energy into electric energy must be the unique character of the interaction between the π-electrons in the main molecular corn and sulfo groups. As mentioned above, the resonance effects: mesomeric and inductive ones could be involved. The individual sulfo group has electron-withdrawing character, however when it is bonded to the phthalocyanine dye there is an interaction between the molecular orbital of the π-electron system and substitutes [59] and it can lead to enhancement of photoactivity of the dyes and the photocurrent. An inductive effect cannot be neglected. However, if we take into consideration electrostatic repulsion between the sulfo groups and the π-electrons of the macroring we could expect to the photocurrent to decrease. However, it is not the case for **2**. It means that for sample **2** the mesomeric effect is much stronger than the inductive one. Of course, the mesomeric effects cannot be excluded in **3** and **4**, since these dyes contain three and four sulfo groups, respectively. Thus, in the case of dye **3** (and **4**) with more sulfo groups than in **2** the lower values of photocurrent can be explained as due to domination of the inductive effects over the mesomeric one. The domination of the mesomeric effects was also widely discussed in copper and zinc phthalocyanines substituted with the electronegative fluorine and chlorine atoms [11,12].

Interactions between electron donor dyes and a semiconductor electrode in PEC can also depend on other effects [9,12,60–63]. The influence of the molecular structure on dye photoactivity as an electron donor has been shown in numerous papers (e.g. [4,9]). Deformation of the molecular skeleton and steric effects leading to changes in conformation of a molecule could also influence photoactivity of the dyes in photocurrent generation [12,64]. The occurrence of steric effects is supported by our photothermal experiments. Photocurrent can be also affected by redox potential of the dyes [60–63] and the presence of counterions [62,65]. However, in this paper our general idea is to show the influence (or not) of the sulfo groups on photocurrent generation. In our paper we want to show weather or not sulfo group(s) is(are) able to affect photoelectric behavior, without going deeply into all mechanisms governing the phenomenon which has been a subject of numerous of papers [9,64,66].

Now the question arises as to the point (v) mentioned above in the previous Section 3.3, that means the perturbation in electron distribution due to intermolecular electron transfer occurring in

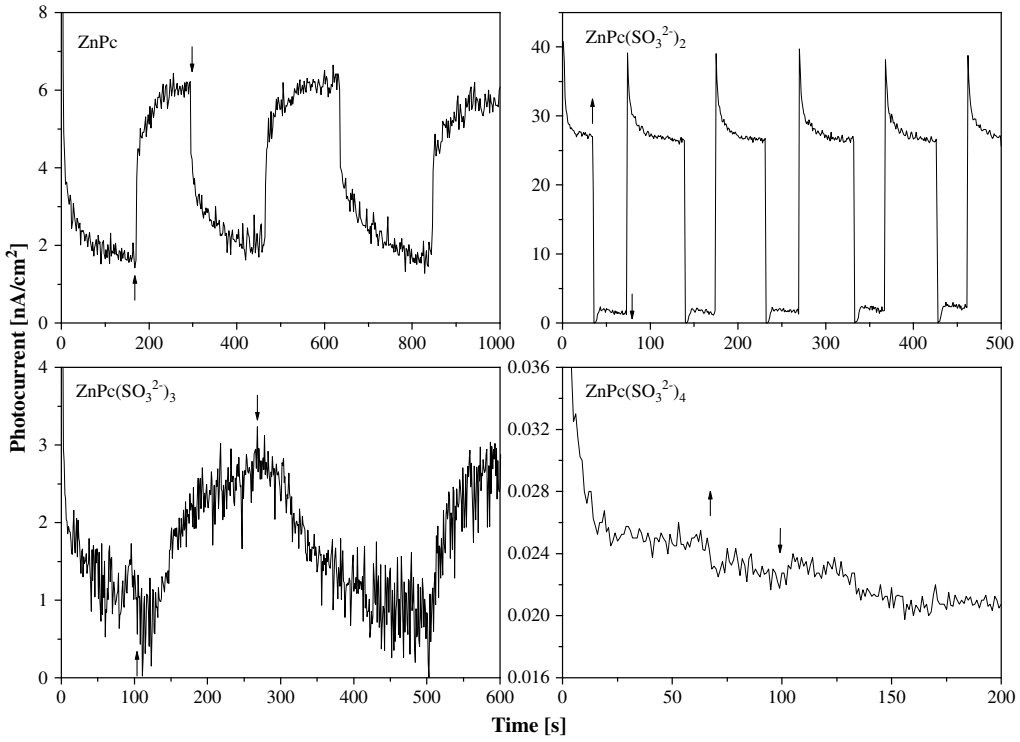

Fig. 7. Kinetics of photocurrent generated in the photoelectrochemical cell with zinc phthalocyanine (ZnPc) and sulfonated zinc phthalocyanines ($ZnPc(SO_3^{2-})_{2-4}$) in DMSO; ($c = 10^{-3}$ M).

the dyes with the sulfo groups attached. The occurrence of this electron transfer has been essentially confirmed by our photoelectric investigation in PEC. Photoelectric study evidently shows enhancement of photocurrent for the dye with two sulfo groups as due to the mesomeric effect. This effect is closely connected with redistribution of the electron cloud in the molecular frame and explains (v). The fluorescence quantum yields of the studied dyes are 0.12–0.16 as found for other phthalocyanine dyes [11]. On the basis of the PAS examination we indicate that part of the energy absorbed is thermally deactivated, however, the LIOAS experiment shows that other non-radiative processes must be involved in the molecules under illumination. Thus, taking into account radiative and non-radiative processes occurring in our samples and the LIOAS and photoelectric results we have a reason to believe that charge separation process occurs with high efficiency. Thus (v) and charge separation processes in our dyes could also explain why the sum of $(k_1 + k_2)$ is not equal to1.

4. Conclusions

On the basis of our spectroscopic experiments (absorption, fluorescence, photoacoustics, LIOAS) and photoelectric examinations performed for zinc phthalocyanines substituted with the sulfo groups we can draw the following conclusions.

1. Sulfonation of zinc phthalocyanine changes markedly absorption and fluorescence properties due to strong redistribution of the electron density in the molecular macroring occurring as a result of the mesomeric and inductive effects, although other effects cannot be excluded.
2. Both singlet and triplet states of the sulfonated phthalocyanine are involved in thermal deactivation.
3. Population of the triplet state depends on the kind of phthalocyanine and number of sulfo groups.
4. Photocurrent enhancement in the phthalocyanine with two sulfo groups could support occurrence of the mesomeric effect which dominates over the inductive one, whereas in phthalocyanine with three and four sulfo groups the inductive effect is essential and can lead to photocurrent declining.

We have shown that sulfonated phthalocyanine dyes can potentially be used as good photoconverters in organic photovoltaics as some of them show efficient photocurrent generation.

Acknowledgements

The paper has been supported by the Ministry of Science and Higher Education as the research projects in the years 2008–2011 DW, Poland and Poznan University of Technology DS-176/2009.

References

[1] Boxer SG. In: Deisenhofer J, Norris JR, editors. The photosynthetic reaction center, vol. 2. Academic Press; 1993. p. 179–220.
[2] Moan J. Porphyrin photosensitization and phototherapy. Photochem Photobiol 1986;43:681–90.
[3] Rosenthal I. Phthalocyanines as photodynamic sensitizers. Photochem Photobiol 1991;53:859–70.
[4] Leznoff CC, Lever ABP. Phthalocyanines: properties and applications. New York: VCH; 1996.
[5] Imahori H, Mori Y, Matano Y. Nanostructured artificial photosynthesis. J Photochem Photobiol C Photochem Rev 2003;4:51–83.
[6] Edrei R, Gottfried V, Van Lier JE, Kimel S. Sulfonated phthalocyanines: photophysical properties, in vitro cell uptake and structure–activity relationships. J Porphyrins Phthalocyanines 198;2:191–199.
[7] Weber JH, Busch DH. Complexes derived from strong ligands. XIX. Magnetic properties of transition metal derivatives of 4,4',4'',4'''–tetrasulfophthalocyanine. Inorg Chem 1965;4:469–71.
[8] Wróbel D, Łukasiewicz J, Goc J, Waszkowiak A, Ion R. Photocurrent generation in an electrochemical cell with substituted metalloporphyrins. J Mol Struct 2000;555:407–17.
[9] Wróbel D. Organic photovoltaic solar cells: spectroscopic and photoelectric properties of photoactive dyes. CR Chemie 2003;6:417–29.

[10] Wróbel D, Dudkowiak A. Porphyrins and phthalocyanines – functional molecular materials for optoelectronic and medicine. Mol Cryst Liq Cryst 2006;448:15–38.
[11] Wróbel D, Boguta A. Study of the influence of substituents on spectroscopic and photoelectric properties of zinc phthalocyanines. J Photochem Photobiol A Chem 2002;150:67–76.
[12] Siejak A, Wróbel D, Ion RM. Study of resonance effects in copper phthalocyanines. J Photochem Photobiol A Chem 2006;181:180–7.
[13] Bonnet R, Harriman A, Kozyrev AN. Photophysics of halogenated porphyrins. J Chem Phys Soc Faraday Trans 1992;88:763–9.
[14] Perry JW, Monsour K, Marder SR, Perry KJ, Alwarez D, Choong I. Enhanced reverse saturable absorption and optical limiting in heavy-atom-substituted phthalocyanines. Optics Lett 1994;19:625–7.
[15] Perry JW, Monsour K, Lee IYS, Bedworth PV, Chen CT, Ng D, et al. Organic optical limiter with a strong nonlinear absorptive response. Science 1996;273:1533–6.
[16] Türker L. Zinc octahalotetraphenylporphyrins – AM1 treatment. J Mol Struct 2001;540:69–77.
[17] Lumbroso H, Amato ME, Lombardo GM, Grassi A. Mesomeric and π-moments in some hetero-conjugated compounds. J Mol Struct 1998;442:183–94.
[18] Lumbroso H. A critical survey on the mesomeric moments of nitrogen-oxide compounds. J Mol Struct 1997;412:181–96.
[19] Gineityte V. Interpretation of the inductive effect of heteroatoms in substituted alkanes on the basis of both the one-electron density matrix and localized molecular orbitals. J Mol Struct 1996;364:85–96.
[20] Cherkasov AR, Galkin VI, Cherkasov RA. 'Inductive' electronegativity scale. J Mol Struct 1999;486:43–6.
[21] Cherkasov AR, Galkin VI, Cherkasov RA. "Inductive" electronegativity scale: 2. 'Inductive' analog of chemical hardness. J Mol Struct 2000;497:115–21.
[22] Vereshtchagin AN. The inductive effect. Moscow: Nauka; 1987.
[23] Cherkasov AR, Galkin VI, Cherkasov RA. A new approach to the theoretical estimation of inductive constants. J Phys Org Chem 1998;11:437–47.
[24] Bociocchi E, d'Acunzo F, Galli C. Steric effects and selectivity in the benzylic hydroxylation by metalloporphyrins and by the fungus *Mortierella isabellina*. Teatrahedron Lett 1995;36:315–8.
[25] Smart BE. Fluorine substituent effects (on bioactivity). J Fluorine Chem 2001;109:3–11.
[26] Ambroz M, Beeby A, MacRobert AJ, Simpson MS, Svensen RK, Phillips D. Preparative, analytical and fluorescence spectroscopic studies of sulphonated aluminium phthalocyanine photosensitisers. J Photochem Photobiol B Biol 1991;9:87–95.
[27] Dixon DW, Gill AF, Sook BR. Characterization of sulfonated phthalocyanines by mass spectrometry and capillary electrophoresis. J Porphyrins Phthalocyanines 2004;8:1300–10.
[28] Lutsenko OG, Shaposhnikov GP, Kulinich VP, Lyubimtsev AV. Synthesis and properties of sulfophenyl-substituted metal phthalocyanine complex. Russian J General Chem 2004;74:446–50.
[29] Humuryudan E, Bayir ZA, Bekaroglu Ö. Dioxadiaza macrocycle-substituted phthalocyanine. Dyes Pigments 1999;43:77–81.
[30] Gordon AJ, Ford RA. The chemist's companion. New York: Wiley; 1972.
[31] Lakowicz J. Principle of fluorescence spectroscopy. New York: Plenum Press; 1999.
[32] Van Zandvoort MAMJ, Wróbel D, Lettinga P, Van Ginkel G, Levine YK. The orientation of the transition dipole moments of chlorophyll alpha and pheophytin alpha in their molecular frame. Photochem Photobiol 1995;62:279–89.
[33] Ducharme D, Tessier A, Leblanc RM. Design and characteristics of a cell for photoacoustic spectroscopy of condensed matter. Rev Sci Instrum 1979;50:1461–2.
[34] Pineiro M, Carvalho AL, Pereira MM, d'A. Rocha AM, Gonsalves AMR, Arnaut LG, et al. Photoacoustic measurements of porphyrin triplet-state quantum yields and singlet-oxygen efficiencies. Chem Eur J 1998;4:2299–307.
[35] Dudkowiak A, Teślak E, Habdas J. Photophysical studies of tetratolylporphyrin photosensitizers for potential medical applications. J Mol Structr 2006;792–793:93–8.
[36] Marti C, Jurgens O, Cuenca O, Casals M, Nonell S. Aromatic ketones as standards for singlet molecular oxygen O2($^1\Delta_g$) photosensitization. Time-resolved photoacoustic and near-IR emission studies. J Photochem Photobiol A 1996;97:11–8.
[37] Rudzki-Small J, Libertini LJ, Small EW. Analysis of photoacoustic waveforms using the nonlinear least squares method. Biophys Chem 1992;42:29–48.
[38] Wróbel D, Boguta A, Ion RM. Spectroscopic and photoelectric studies of phthalocyanine in polyvinyl alcohol for application in solar energy conversion. Int J Photoenerg 2000;2:87–96.
[39] Davis RC, Ditson SL, Fentiman AF, Pearlstein RM. Reversible wavelength shifts of chlorophyll induced by a point charge. J Am Chem Soc 1981;106:6823–6.
[40] Katz JJ, Shipman LL, Cotton TM, Janson TR. In: Dolphin D, editor. Porphyrins, vol. V. New York: Academic; 1978. p. 402–58.
[41] Warshel AJ. On the origin of the red shift of the absorption spectra of aggregated chlorophylls. J Am Chem Soc 1979;101:744–6.
[42] Speirs NM, Ebenezer WJ, Jones AC. Observation of a fluorescence dimer of a sulfonated phthalocyanine. Photochem Photobiol 2002;76:241–68.
[43] Kudrevich S, Brasseur N, La Madeleine C, Gilbert S, van Lier JE. Syntheses and photodynamic activities of novel trisulfonated zinc phthalocyanine derivatives. J Med Chem 1997;40:3897–904.
[44] Yang YC, Ward JR, Seiders RP. Dimerization of cobalt(II) tetrasulfonated phthalocyanine in water and aqueous alcoholic solutions. Inorg Chem 1985;24:1765–9.
[45] Marais E, Klein R, Antunes E, Nyokong T. Photocatalysis of 4-nitrophenol using zinc phthalocyanines complexes. J Mol Catalysis A Chem 2007;261:36–42.
[46] Brożek-Płuska B, Szymczyk I, Abramczyk H. Raman spectroscopy of phthalocyanines and their sulfonated derivatives. J Mol Struct 2005;744–747:481–5.
[47] Gottstein J, Scheer H. Long-wavelength-absorbing forms of bacteriochlorophyll solutions of Triton X-100. Proc Natl Acad Sci U S A 1982;80:2231–4.
[48] Agostino A, Catucci L, Colafemmina G, Scheer H. Role of functional groups and surfactant charge in regulating chlorophyll aggregation in micellar solutions. J Phys Chem B 2002;106:1446–54.
[49] Shepanski JF, Knox RS. Circular dichroism and other optical properties of antenna chlorophyll proteins from higher plants. Israel J Chem 1981;21:325–34.
[50] Thornber JP, Trosper TL, Strouse CE. In: Clayton RK, Sistrom WR, editors. The photosynthetic bacteria. New York: Plenum Press; 1978. p. 133.
[51] Abramczyk H, Szymczyk I, Waliszewska G, Lebioda A. Photoinduced redox processes in phthalocyanine derivatives by resonance Raman spectroscopy and time resolved techniques. J Phys Chem A 2004;108:264–74.
[52] Abramczyk H, Brożek-Płuska B, Karczewski K, Karczewska M, Szymczyk I, Krzyczmonik P, et al. Femtosecond transient absorption, Raman and electrochemistry studies of tetrasulphonated copper phthalocyanine in water solutions. J Phys Chem A 2006;110:8627–36.
[53] Nawrocka A, Krawczyk S. Electronic excited state of alizarin dye adsorbed on TiO_2 nanoparticles: a study by electroabsorption (Stark effect) spectroscopy. J Phys Chem 2008;112:10233–41.
[54] Rosencwaig A. Photoacoustics and photoacoustic spectroscopy. New York: Wiley; 1980.
[55] Laurence DS, Witten DW. Photochemistry and photophysical properties of novel, unsymmetrically substituted metallophthalocyanines. Photochem Photobiol 1996;64:923–35.
[56] Wróbel D, Łukasiewicz J, Boguta A. The interportance of non-radiative processes in porphyrins and phthalocyanines for photocurrent generation study. J Phys IV 2003;109:111–21.
[57] Azenha EG, Serra AC, Pineiro M, Pereira MM, de Melo JS, Arnaut LG, et al. Heavy-atom effects on metalloporphyrins and polyhalogenated porphyrins. Chem Phys 2002;280:177–90.
[58] Wróbel D, Łukasiewicz J, Manikowski H. Fluorescence quenching and ESR spectroscopy of metallic porphyrins in the presence of an electron acceptor. Dyes Pigments 2003;58:7–18.
[59] Kerber RC. If it's resonance, what is resonating? J Chem Educ 2006;83:223–7.
[60] Zhang LY, Frisner RA. Ab initio electronic structure calculation of redox potentials of bacteriochlorophyll and bacteriopheophytin in solution. J Phys Chem 1995;99:16479–82.
[61] Lenza RO, Juanto S, Zagal JH. Spectrochemical studies of tetrasulfonated metallophthalocyanines adsorbed on the basal plane of graphite in the presence of cysteine. J Electroanal Chem 1998;452:221–8.
[62] Lever ABP, Wilshire JP. Redox potentials of metal phthalocyanines in non-aqueous media. Can J Chem 1976;54:2514–6.
[63] Daziano J-P, Steenken S, Chabannon C, Mannoni P, Chanon M, Julliard M. Photophysical and redox properties of phthalocyanines: relation with their photodynamic activities on TF-1 and Daudi leukemic cells. Photochem Photobiol 1996;64:712–24.
[64] Garcia CG, Iha NY, Argacci MR, Bignozzi CA. 4-Phenylpyridine as ancillary ligand in ruthenium(II) polypyridyl complexes for sensitization of n-type TiO_2. J Photochem Photobiol A Chem 1998;114:23241–9.
[65] Cheung KM, Bloor D, Stevens CG. The influence of unusual counterions on the electrochemistry and physical properties of polypyrrole. J Mater Sci 1990;25:3814–37.
[66] O'Regan B, Grätzel M. Photovoltaic and photochemical conversion of solar cell Low cost and highly efficient solar cells based on the sensitization of colloidal titanium dioxide. Nature 1991;335:7377–85.
[67] Ogunside A, Nyokong T. Effects of substituents and solvents on the photochemical properties of zinc phthalocyanine complexes and their protonated derivatives. J Mol Struct 2004;689:89–97.